J|A|C|S
ARTICLES

Published on Web 06/18/2008

Reactivity and Infrared Spectroscopy of Gaseous Hydrated Trivalent Metal Ions

Matthew F. Bush, Richard J. Saykally, and Evan R. Williams*

Department of Chemistry, University of California, Berkeley, California 94720-1460

Received March 13, 2008; E-mail: williams@cchem.berkeley.edu

Abstract: Hydrated trivalent rare earth metal ions containing yttrium and all naturally abundant lanthanide metals are formed using electrospray ionization, and the structures and reactivities of these ions containing 17−21 water molecules are probed using blackbody infrared radiative dissociation (BIRD) and infrared action spectroscopy. With the low-energy activation conditions of BIRD, there is an abrupt transition in the dissociation pathway from the exclusive loss of a single neutral water molecule to the exclusive loss of a small protonated water cluster via a charge-separation process. This transition occurs over a narrow range of cluster sizes that differs by only a few water molecules for each metal ion. The effective turnover size at which these two dissociation rates become equal depends on metal ion identity and is poorly correlated with the third ionization energies of the isolated metals but is well correlated with the hydrolysis constants of the trivalent metal ions in bulk aqueous solution. Infrared action spectra of these ions at cluster sizes near the turnover size are largely independent of the specific identity of the trivalent metal ion, suggesting that any differences in the structures of the ions present in our experiment are subtle.

Introduction

The optical properties of lanthanide metals are strongly affected by interactions with water molecules, which makes them useful as luminescent sensors[1,2] and imaging markers.[1,3] For example, the luminescence intensity of Eu^{III} is very sensitive to the identity of coordinating ligands, and changes in coordination with pH enables a dipyridyl-containing cryptate complex to be used as a sensitive probe of solution pH.[2] Maximum luminescent intensity is observed near neutral pH, corresponding to conditions in which the metal ion is fully solvated by amine groups from the cryptate ligand.[2] Luminescence intensity decreases with decreasing pH due to additional interactions with water molecules,[2] which are more effective than amine groups at quenching lanthanide luminescence.[4] Some of the amine groups are protonated under these conditions and no longer solvate the metal ion, which enables additional interactions between water molecules and the metal ion.[2] With increasing pH, Eu^{III} luminescence in the cryptate complex is quenched by hydroxide ligands formed via hydrolysis.[2] Another important application of lanthanide metal ions is the use of Gd^{III} in MRI contrast agents.[5,6] Gd^{III} shortens the relaxation times of neighboring water molecules, which increases the contrast with water molecules in neighboring tissues.[5,6] Chelation of Gd^{III} is necessary because the pure aqua ion is highly toxic in vivo, but chelation reduces the MRI contrast because fewer water molecules interact with the metal ion and these water molecules typically exchange more slowly with outer-shell water molecules.[5,6] A more detailed understanding of lanthanide metal ion solvation, dynamics and reactivity may enable the development of new lanthanide-containing complexes with optimized interactions with water molecules.

Gas-phase studies of microsolvated ions can provide detailed information about the structures, stabilities, relative solvent affinities, and reactivities of ions,[7–12] but studying hydrated multiply charged metal ions in the gas phase is particularly challenging due to the potential for a competing charge-separation reaction in which both products are charged. For example, $[Ca(H_2O)]^{2+}$ is readily formed by condensation, but the addition of a second water molecule to this cluster results in the formation of the metal hydroxide with one less net charge and a protonated water molecule (Reaction 1):[13,14]

$$[Ca(H_2O)]^{2+} + H_2O \rightarrow [Ca(OH)]^{+} + H_3O^{+} \qquad (1)$$

(1) Bünzli, J. C. G.; Piguet, C. *Chem. Soc. Rev.* **2005**, *34*, 1048–1077.
(2) Bazzicalupi, C.; Bencini, A.; Bianchi, A.; Giorgi, C.; Fusi, V.; Masotti, A.; Valtancoli, B.; Roque, A.; Pina, F. *Chem. Commun.* **2000**, 561–562.
(3) Weibel, N.; Charbonniere, L. J.; Guardigli, M.; Roda, A.; Ziessel, R. *J. Am. Chem. Soc.* **2004**, *126*, 4888–4896.
(4) Beeby, A.; Clarkson, I. M.; Dickins, R. S.; Faulkner, S.; Parker, D.; Royle, L.; de Sousa, A. S.; Williams, J. A. G.; Woods, M. *J. Chem. Soc., Perkin Trans. 2* **1999**, 493–503.
(5) Caravan, P.; Ellison, J. J.; McMurry, T. J.; Lauffer, R. B. *Chem. Rev.* **1999**, *99*, 2293–2352.
(6) Raymond, K. N.; Pierre, V. C. *Bioconjugate Chem.* **2005**, *16*, 3–8.
(7) Chang, H. C.; Wu, C. C.; Kuo, J. L. *Int. Rev. Phys. Chem.* **2005**, *24*, 553–578.
(8) Shin, J. W.; Hammer, N. I.; Diken, E. G.; Johnson, M. A.; Walters, R. S.; Jaeger, T. D.; Duncan, M. A.; Christie, R. A.; Jordan, K. D. *Science* **2004**, *304*, 1137–1140.
(9) Miyazaki, M.; Fujii, A.; Ebata, T.; Mikami, N. *Science* **2004**, *304*, 1134–1137.
(10) Asmis, K. R.; Santambrogio, G.; Zhou, J.; Garand, E.; Headrick, J.; Goebbert, D.; Johnson, M. A.; Neumark, D. M. *J. Chem. Phys.* **2007**, *126*, 191105.
(11) Walters, R. S.; Pillai, E. D.; Duncan, M. A. *J. Am. Chem. Soc.* **2005**, *127*, 16599–16610.
(12) Kolaski, M.; Lee, H. M.; Choi, Y. C.; Kim, K. S.; Tarakeshwar, P.; Miller, D. J.; Lisy, J. M. *J. Chem. Phys.* **2007**, *126*, 074302.
(13) Beyer, M.; Williams, E. R.; Bondybey, V. E. *J. Am. Chem. Soc.* **1999**, *121*, 1565–1573.
(14) Spears, K. G.; Fehsenfe, K. C. *J. Chem. Phys.* **1972**, *56*, 5698–5705.

10.1021/ja801894d CCC: $40.75

Charge-separation reactions can prevent the formation of larger, more highly charged cluster ions by condensation in supersonic expansions. A different strategy to form these ions is through evaporation from more extensively solvated ions using methods such as thermospray[15] or electrospray (ESI).[16–21] Alternatively, neutral ligated clusters formed in supersonic expansions can be subsequently ionized via electron impact.[22,23] Many hydrated divalent metal ions and dianions have been observed using these techniques, enabling characterization using a variety of methods, including high-pressure mass spectrometry (HPMS),[16,24–26] blackbody infrared radiative dissociation (BIRD),[19,27–29] electronic spectroscopy,[30] ion molecule reactions,[18] photoelectron spectroscopy,[31] guided ion beam mass spectrometry,[21] electron capture,[32–34] and infrared action spectroscopy.[35–37]

Although clusters of trivalent metal ions with dimethylsulfoxide, dimethylformamide, acetonitrile, diacetonealcohol, and other ligands have been observed in the gas phase,[22,38–45] early attempts to form analogous complexes with water were not successful. For example, under conditions in which ESI from solutions containing divalent metal ion salts readily yield $[M(H_2O)_n]^{2+}$ ions, solutions containing trivalent metal ion salts instead yield charge-reduced ions of the form $[M(OH)(H_2O)_n]^{2+}$.[24,26,38] Using ESI, $[M(H_2O)_n]^{3+}$ ions were recently observed for M = La, Ce, and Eu, and initial experiments suggest that nanometer-scale droplets are necessary to prevent charge reduction.[20] Ions of M = La, Tb, and Lu were subsequently observed by McQuinn et al. in ESI experiments performed on a commercial instrument, although the resulting mass spectra were "dominated by abundant $[H(H_2O)_n]^+$ clusters".[46]

Activation of hydrated multiply charged cations can result in dissociation by two different pathways depending on cluster size and experimental conditions: loss of a neutral water molecule (Reaction 2) or proton transfer to form a reduced charge metal hydroxide and a protonated water molecule or cluster (Reaction 3):[13,16,17,47]

$$[M(H_2O)_n]^{x+} \rightarrow [M(H_2O)_{n-1}]^{x+} + H_2O \quad (2)$$

$$[M(H_2O)_n]^{x+} \rightarrow [M(OH)(H_2O)_{n-m-1}]^{(x-1)+} + H^+(H_2O)_m \quad (3)$$

For large clusters, loss of a water molecule is the favorable process. For smaller clusters, charge-separation reactions become competitive and can ultimately dominate as the cluster size decreases. The branching ratio for these two competitive dissociation channels depends on the extent of hydration, the metal ion identity, and experimental parameters. For example, with BIRD, a low-energy activation method, $[Cu(H_2O)_n]^{2+}$ dissociates via Reaction 2 for $n > 8$, via Reaction 3 for $n < 8$, and both processes are observed for $n = 8$.[47] With collisional activation, which can deposit more internal energy than BIRD, Reaction 2 is favored and $[Cu(H_2O)]^{2+}$ can be formed from $[Cu(H_2O)_7]^{2+}$ using a 128 eV laboratory reference frame collision energy with argon gas.[17] This indicates that Reaction 2 is entropically favored compared to Reaction 3 in this size range. Factors that affect the minimum number of water molecules that are necessary to stabilize divalent ions are discussed elsewhere.[13,16,17]

Here we report the observation of hydrated trivalent rare earth metals ion clusters containing yttrium and all naturally abundant lanthanide metals. The special reactivities of these ions are probed with BIRD, both as a function of metal ion identity and as the number of water molecules, revealing an abrupt transition in dissociation behavior with decreasing cluster size. The structures of hydrated trivalent metal ions near this critical size are probed with infrared action spectroscopy. These are the first studies to probe the reactivity of size-selected hydrated trivalent metals ions in a range where a transition in reactivity occurs and comprise the first use of spectroscopy to probe their structures.

Experimental Section

Experiments were performed on the Berkeley 2.75 T Fourier-transform ion cyclotron resonance mass spectrometer.[48] Hydrated ions were formed by nanospray ionization using a home-built

(15) Schmelzeisenredeker, G.; Bütfering, L.; Röllgen, F. W. *Int. J. Mass Spectrom. Ion Processes* **1989**, *90*, 139–150.
(16) Peschke, M.; Blades, A. T.; Kebarle, P. *Int. J. Mass Spectrom.* **1999**, *187*, 685–699.
(17) Shvartsburg, A. A.; Siu, K. W. M. *J. Am. Chem. Soc.* **2001**, *123*, 10071–10075.
(18) Rodriguez-Cruz, S. E.; Williams, E. R. *J. Am. Soc. Mass Spectrom.* **2001**, *12*, 250–257.
(19) Wong, R. L.; Paech, K.; Williams, E. R. *Int. J. Mass Spectrom.* **2004**, *232*, 59–66.
(20) Bush, M. F.; Saykally, R. J.; Williams, E. R. *Int. J. Mass Spectrom.* **2006**, *253*, 256–262.
(21) Carl, D. R.; Moision, R. M.; Armentrout, P. B. *Int. J. Mass Spectrom.* **2007**, *265*, 308–325.
(22) Walker, N. R.; Wright, R. R.; Stace, A. J.; Woodward, C. A. *Int. J. Mass Spectrom.* **1999**, *188*, 113–119.
(23) Duncombe, B. J.; Duale, K.; Buchanan-Smith, A.; Stace, A. J. *J. Phys. Chem. A* **2007**, *111*, 5158–5165.
(24) Blades, A. T.; Jayaweera, P.; Ikonomou, M. G.; Kebarle, P. *Int. J. Mass Spectrom. Ion Processes* **1990**, *102*, 251–267.
(25) Blades, A. T.; Kebarle, P. *J. Phys. Chem. A* **2005**, *109*, 8293–8298.
(26) Blades, A. T.; Jayaweera, P.; Ikonomou, M. G.; Kebarle, P. *J. Chem. Phys.* **1990**, *92*, 5900–5906.
(27) Rodriguez-Cruz, S. E.; Jockusch, R. A.; Williams, E. R. *J. Am. Chem. Soc.* **1998**, *120*, 5842–5843.
(28) Rodriguez-Cruz, S. E.; Jockusch, R. A.; Williams, E. R. *J. Am. Chem. Soc.* **1999**, *121*, 8898–8906.
(29) Wong, R. L.; Williams, E. R. *J. Phys. Chem. A* **2003**, *107*, 10976–10983.
(30) Faherty, K. P.; Thompson, C. J.; Aguirre, F.; Michne, J.; Metz, R. B. *J. Phys. Chem. A* **2001**, *105*, 10054–10059.
(31) Wang, X.-B.; Yang, J.; Wang, L.-S. *J. Phys. Chem. A* **2008**, *112*, 172–175.
(32) Leib, R. D.; Donald, W. A.; Bush, M. F.; O'Brien, J. T.; Williams, E. R. *J. Am. Chem. Soc.* **2007**, *129*, 4894–4895.
(33) Leib, R. D.; Donald, W. A.; Bush, M. F.; O'Brien, J. T.; Williams, E. R. *J. Am. Soc. Mass Spectrom.* **2007**, *18*, 1217–1231.
(34) Donald, W. A.; Leib, R. D.; O'Brien, J. T.; Bush, M. F.; Williams, E. R. *J. Am. Chem. Soc.* **2008**, *130*, 4879–4885.
(35) Zhou, J.; Santambrogio, G.; Brümmer, M.; Moore, D. T.; Wöste, L.; Meijer, G.; Neumark, D. M.; Asmis, K. R. *J. Chem. Phys.* **2006**, *125*, 111102.
(36) Bush, M. F.; Saykally, R. J.; Williams, E. R. *ChemPhysChem* **2007**, *8*, 2245–2253.
(37) Bush, M. F.; Saykally, R. J.; Williams, E. R. *J. Am. Chem. Soc.* **2007**, *129*, 2220–2221.
(38) Blades, A. T.; Jayaweera, P.; Ikonomou, M. G.; Kebarle, P. *Int. J. Mass Spectrom. Ion Processes* **1990**, *101*, 325–336.
(39) El-Nahas, A. M.; Xiao, C. Y.; Hagelberg, F. *Int. J. Mass Spectrom.* **2004**, *237*, 47–54.
(40) Kojima, T.; Kudaka, I.; Sato, T.; Asakawa, T.; Akiyama, R.; Kawashima, Y.; Hiraoka, K. *Rapid Commun. Mass Spectrom.* **1999**, *13*, 2090–2097.
(41) Puskar, L.; Tomlins, K.; Duncombe, B.; Cox, H.; Stace, A. J. *J. Am. Chem. Soc.* **2005**, *127*, 7559–7569.
(42) Shvartsburg, A. A. *J. Am. Chem. Soc.* **2002**, *124*, 12343–12351.
(43) Shvartsburg, A. A. *Chem. Phys. Lett.* **2002**, *360*, 479–486.
(44) Shvartsburg, A. A. *J. Am. Chem. Soc.* **2002**, *124*, 7910–7911.
(45) Shi, T. J.; Hopkinson, A. C.; Siu, K. W. M. *Chem. - Eur. J.* **2007**, *13*, 1142–1151.
(46) McQuinn, K.; Hof, F.; McIndoe, J. S. *Chem. Commun.* **2007**, *40*, 4099–4101.
(47) O'Brien, J. T.; Williams, E. R. J. Phys. Chem. A 2008, in press.
(48) Bush, M. F.; O'Brien, J. T.; Prell, J. S.; Saykally, R. J.; Williams, E. R. *J. Am. Chem. Soc.* **2007**, *129*, 1612–1622.

interface described elsewhere.[20] The copper block surrounding the stainless steel capillary entrance to the mass spectrometer was maintained at 90−95 °C.[20] Electrospray solutions were made to ~1 mM of the trivalent metal ion of interest, typically using hexahydrated metal chloride salts from commercial sources, in ultrapure water (18.2 MΩ, ≤4 ppb organic content) from a Milli-Q Gradient water purification system. Ions were accumulated for 3−10 s in a cylindrical ion cell that is surrounded by a copper jacket cooled to 130 or 220 K using a regulated flow of liquid nitrogen.[19] To assist with ion trapping and thermalization, dry N_2 gas is introduced into the ion cell at a pressure of $\sim 10^{-6}$ Torr using a piezoelectric valve during ion accumulation. A delay of 15−35 s, during which time residual gases are pumped out to a cell pressure $<10^{-8}$ Torr,[49] allows ions to undergo activation by BIRD so that the hydrated ion distributions generated by electrospray shift to smaller cluster sizes. Infrared action-spectroscopy experiments were performed using light generated by a tunable infrared optical parametric oscillator/amplifier (LaserVision, Bellevue, WA), which yielded ~60 mW of light with ~3 cm^{-1} bandwidth over the frequency range of interest. Infrared frequencies were calibrated by measuring the action spectrum of $H^+(H_2O)_{21}$ and comparing this spectrum to that reported previously for this ion.[8]

Results and Discussion

Formation of Hydrated Trivalent Metal Ions. Hydrated ions in an ESI mass spectrum can be formed by evaporation of water molecules from larger hydrated precursor ions and by condensation of water molecules onto smaller hydrated ions.[50] Previous results indicate that maintaining nanometer-scale droplets through the entire ESI process is essential to preserving the charge states of hydrated trivalent metal ions.[20] The abundance of $[M(H_2O)_n]^{3+}$ is generally greatest for larger values of n, e.g., $n > 100$. Attempts to shift the distribution of $[M(H_2O)_n]^{3+}$ to smaller n by using "harsher" conditions in the nanospray interface generally resulted in increased abundances of $[M(OH)(H_2O)_n]^{2+}$ at the expense of that for $[M(H_2O)_n]^{3+}$. Smaller clusters can be formed by dissociation of larger clusters in the higher pressure source region, and then undergo a charge-separation reaction. Water can subsequently condense on these lower-charge-state ions during the supersonic expansion that occurs in the transition from high to low pressure in the interface.[20,50] High abundances of $[M(H_2O)_n]^{3+}$ with substantially smaller values of n, e.g., $n \approx 20-40$, could be generated by allowing larger clusters, e.g., $n > 100$, to gently evaporate over the course of 15−35 s as a result of BIRD. The integrated infrared cross sections of these ions should be roughly proportional to n due to the increased number of oscillators,[51–53] but threshold dissociation energies depend only weakly on n,[34] such that larger clusters dissociate preferentially. A representative mass spectrum obtained by trapping ions formed by ESI of $LaCl_3 \cdot (H_2O)_6$ and subsequent dissociation by BIRD for 30 s to obtain smaller clusters is shown in Figure 1A. Because of the long ion storage time and low pressure, the ions should reach a steady-state internal energy distribution that is determined by the temperature of the copper jacket surrounding the ion cell through radiation absorption and emission, as well as by evaporative cooling.[52,53]

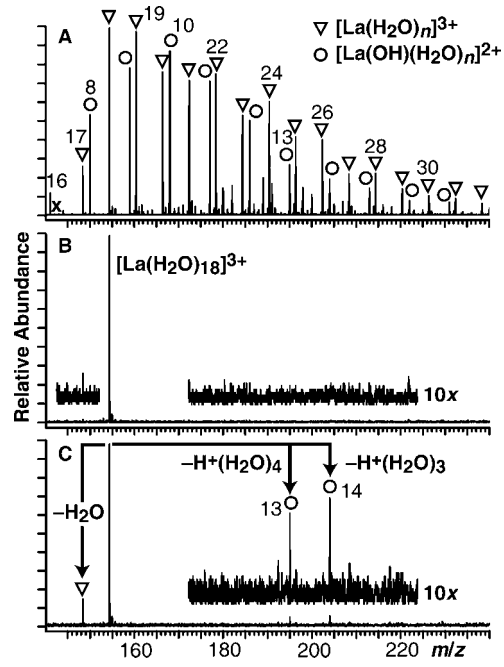

Figure 1. ESI mass spectrum of a solution of 1 mM $LaCl_3$ obtained at a copper jacket temperature of 220 K and a BIRD delay of 30 s to produce smaller clusters (A), isolated $[La(H_2O)_{18}]^{3+}$ (B), and a product spectrum resulting from 1 s BIRD of $[La(H_2O)_{18}]^{3+}$ (C).

$[M(H_2O)_n]^{3+}$ ions were observed for yttrium and all naturally abundant lanthanide metals using this approach. Ion intensities were adequate to enable dissociation experiments for all metals except M = Yb; intensities for this lanthanide were at least an order of magnitude weaker than those for the remaining M. Under conditions that readily yielded $[M(H_2O)_n]^{3+}$ for the remaining M, $[Yb(H_2O)_n]^{3+}$ intensities were <1% of the total ion signal in ESI mass spectra; intense signals for $[Yb(OH)(H_2O)_n]^{2+}$ were observed instead. The low signal observed for $[Yb(H_2O)_n]^{3+}$ precluded additional characterization of these ions.

Dissociation Pathways. BIRD at a copper jacket temperature of 220 K of $[La(H_2O)_n]^{3+}$, $n \geq 19$, results exclusively in the loss of a single neutral water molecule (Reaction 2), whereas BIRD of $[La(H_2O)_{17}]^{3+}$ results exclusively in charge separation (Reaction 3). BIRD of $[La(H_2O)_{18}]^{3+}$ results in dissociation via both pathways to form $[La(H_2O)_{17}]^{3+}$, $[La(OH)(H_2O)_{13}]^{2+}$, $[La(OH)(H_2O)_{14}]^{2+}$, $[H(H_2O)_3]^+$, and $[H(H_2O)_4]^+$ (Figure 1C). One second BIRD reaction times were used to ensure that any subsequent depletion of product ions through either of these two reactions is minimized. Protonated water cluster products were not directly measured in most experiments in order to optimize instrument detection conditions for the higher m/z ions. The intensities of these products were instead estimated as 1/2 those of the corresponding $[M(OH)(H_2O)_n]^{2+}$ products, which accounts for the different charge states. Formation of the protonated water cluster products was confirmed by additional experiments in which mass spectra were also obtained for lower m/z values.

Similar experiments were performed for each of the metal ions. The neutral-loss fraction, defined as the fraction of all product ions that are formed via Reaction 2, resulting from 1 s BIRD at a copper jacket temperature of 220 K for precursor

(49) One of the UHV pumps normally used for experiments on this instrument was not functional for some of the spectroscopy experiments, resulting in high base pressures (~3 × 10^{-8} Torr) and an overall reduction in S/N.

(50) Rodriguez-Cruz, S. E.; Klassen, J. S.; Williams, E. R. *J. Am. Soc. Mass Spectrom.* **1999**, *10*, 958–968.
(51) Schindler, T.; Berg, C.; Niedner-Schatteburg, G.; Bondybey, V. E. *Chem. Phys. Lett.* **1996**, *250*, 301–308.
(52) Price, W. D.; Williams, E. R. *J. Phys. Chem. A* **1997**, *101*, 8844–8852.
(53) Price, W. D.; Schnier, P. D.; Jockusch, R. A.; Strittmatter, E. F.; Williams, E. R. *J. Am. Chem. Soc.* **1996**, *118*, 10640–10644.

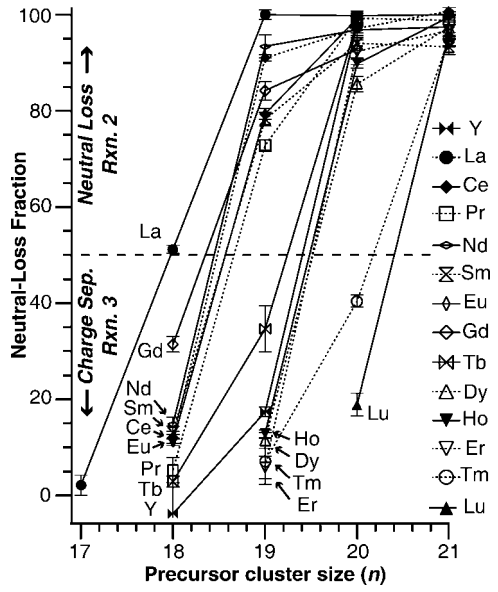

Figure 2. Neutral-loss fractions, defined as the fraction of all product ions that are formed via Reaction 2, measured after 1 s BIRD at a copper jacket temperature of 220 K. Error bars are one standard deviation. Color figure available as Supporting Information Figure 1.

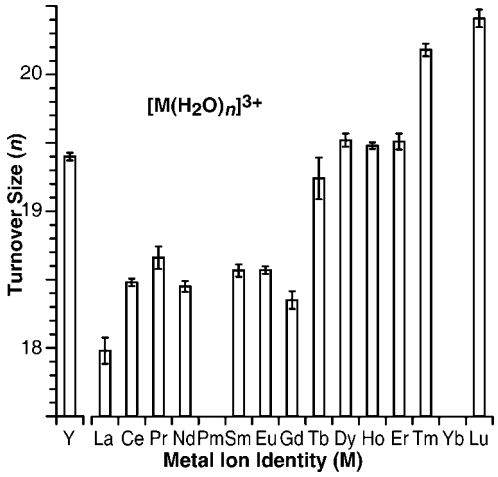

Figure 3. Turnover sizes, defined as the effective cluster size at which the neutral-loss and charge-separation reaction rates become equal, for $[M(H_2O)_n]^{3+}$ determined using the data in Figure 2. Error bars are two standard deviations. Experiments were not performed for M = Pm and Yb.

ions containing M = Y and all naturally occurring lanthanide metals except M = Yb, are plotted as a function of cluster size in Figure 2. The transition between the two dissociation pathways occurs over a narrow range of n (3 or 4) for each M (Figure 2), but there are significant differences in these ranges between the various metal ions studied.

Effect of Trivalent Metal Ion Identity on Dissociation Pathways. An alternative way to compare the reactivity of these hydrated trivalent metal ions is to determine the effective cluster size at which the rates of Reaction 2 and Reaction 3 become equal by finding the intercept between the neutral-loss curves and the line drawn at a neutral-loss fraction of one-half. These values, designated turnover sizes, are shown in Figure 3 and exhibit a strong dependence on metal ion identity.

With BIRD, the smallest $[M(H_2O)_n]^{3+}$ product ions contain 17, 18, and 19 water molecules for M = La, Tb, and Lu,

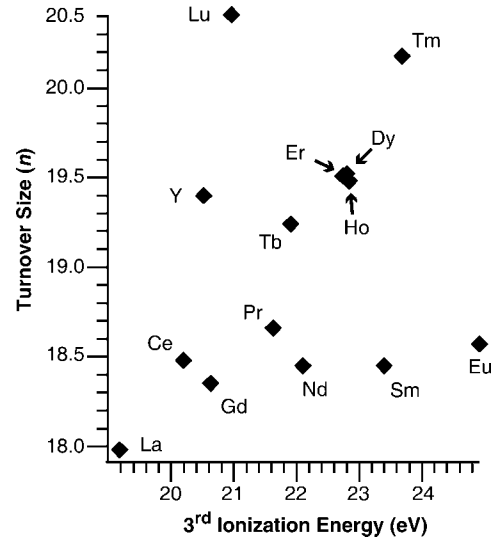

Figure 4. Turnover size plotted versus the third IEs of the isolated metals.

respectively. In contrast, the smallest $[M(H_2O)_n]^{3+}$ products observed by McQuinn et al. from collisionally activated dissociation (CAD) of $[M(H_2O)_{48}]^{3+}$ contained 15, 16, 18 for M = La, Tb, and Lu, respectively.[46] The internal energy deposition in the CAD experiments is considerably greater than that in the BIRD experiments, and comparison of these results indicates that the loss of a neutral water molecule is entropically favored compared to the loss of a protonated water cluster, consistent with analogous results for hydrated sulfate dianions.[29] Because BIRD is a very "gentle" activation method, especially at 220 K, the cluster size at which the transition occurs is likely an upper limit to what would be observed by other activation methods. Significantly smaller $[M(H_2O)_n]^{3+}$ clusters could very likely be generated using more energetic activation methods.

Reactivity and Ionization Energies of the Isolated Metals. Kebarle and others have made pioneering contributions to understanding trends in reactivity for the competitive loss of a neutral water molecule or a protonated water molecule from hydrated divalent metal ions. In a thermochemical cycle reported by Kebarle and co-workers, values for the second ionization energies (IEs) of the metals and hydroxyl binding energies to the singly charged metal ion were determined to have the greatest effect on the observed reactivity of the hydrated divalent metal ions.[24] Many subsequent investigations of $[M \cdot L_n]^{x+}$ ions, where L refers to a solvating ligand, e.g., acetonitrile, dimethylsulfoxide, methanol, or water, demonstrated that several aspects of the formation and reactivity of the these ions were predominantly attributable to the relevant IEs of M and L.[17,22,38,42–44,54,55] In contrast, the present study shows that the turnover sizes of $[M(H_2O)_n]^{3+}$ are not well correlated with the third IEs of the isolated metals (Figure 4). For example, the third IEs of Ce and Eu differ by 4.7 eV and the turnover sizes of the hydrated trivalent metal ions differ by only 0.1 water molecules, whereas the third IEs of Gd and Lu differ by only 0.3 eV and the turnover sizes of these hydrated trivalent metal ions differ by 2.1 water molecules.

Although Kebarle's thermochemical cycle[24] is correct, the $[MOH]^+$ product in that thermochemical cycle is treated as a

(54) Wright, R. R.; Walker, N. R.; Firth, S.; Stace, A. J. *J. Phys. Chem. A* **2001**, *105*, 54–64.
(55) Shvartsburg, A. A.; Wilkes, J. G. *J. Phys. Chem. A* **2002**, *106*, 4543–4551.

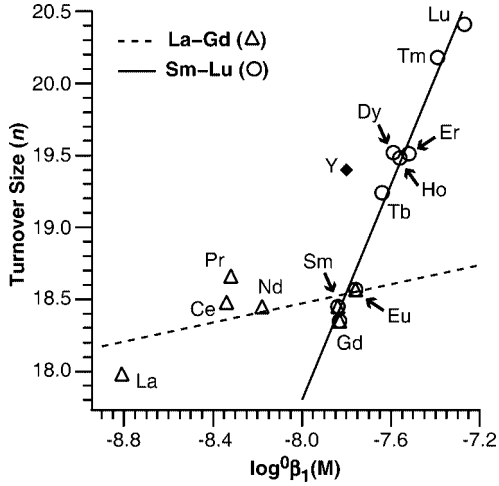

Figure 5. Turnover size plotted versus the first hydrolysis constant, log ${}^0\beta_1$(M),[57] for each trivalent metal ion studied in bulk aqueous solutions. Linear best fits are shown for La−Gd (dashed line) and Sm−Lu (solid line). Note that the elements near the middle of the lanthanide series, Sm, Eu, and Gd, are included with both sets.

singly charged metal ion interacting with a hydroxyl radical, rather than as a divalent metal ion interacting with a hydroxide anion. A modified thermochemical cycle devised by Beyer et al. replaces the terms involving electron transfer with more chemically intuitive terms involving proton transfer.[13] That analysis and calculations exploring the transition state for charge separation indicate that effects of second IEs on the charge-separation chemistry of $[M(H_2O)_2]^{2+}$ ions, M = alkaline earth metals, are indirect.[13]

Another important consideration is that the IEs of metals hydrated in water nanodrops can be considerably different than those in isolation. For example, calculated adiabatic IEs for $[Mg(H_2O)_n]^+$ rapidly decrease from 15 eV for $n = 0$ to 10 eV for $n = 3$.[56] Depending on the level of theory, this value converges to ca. 4−7 eV with increasing n.[56] Electron capture nanocalorimetry experiments indicate that the electron recombination energies for $[M(H_2O)_{32}]^{2+}$ are 4.4,[32] 7.8,[34] and 4.5 eV,[32] for M = Ba, Cu, and Mg, respectively, whereas the second IEs of the isolated metals are 10.0, 20.3, and 15.0 eV. For large hydrated ions such as these, the recombination energies correspond to the adiabatic IEs of the reduced hydrated metal ions.[33,34] In all of these cases, the second IEs of moderately solvated metal ions are considerably less than the IE of a water molecule, consistent with charge-separation reactions from $[M(H_2O)_n]^{3+}$ occurring through proton transfer rather than electron transfer.

Reactivity and the Hydrolysis Constants in Aqueous Solution. Metal-mediated water hydrolysis in aqueous solution (Reaction 4)

$$M^{3+}(aq) + H_2O \rightarrow [MOH]^{2+}(aq) + H^+(aq) \qquad (4)$$

is very similar to the gas-phase charge-separation reaction observed for small $[M(H_2O)_n]^{3+}$ (Reaction 3). Interestingly, the gas-phase turnover sizes for $[M(H_2O)_n]^{3+}$ ions appear to be reasonably well correlated with solution hydrolysis constants[57] (Figure 5). Proceeding across the lanthanide metals series, data for M = La−Gd and Sm−Lu can both be fit well by straight lines. M = Sm, Eu, and Gd can be fit equally well by both lines, and this behavior is generally consistent with a "gadolinium break."

Many aspects of the coordination chemistry and reactivity of the lanthanide metals have transitions in the middle of the series that are often referred to as "gadolinium breaks." For complexes with the same coordination number (CN), the ionic radii of the lanthanide metals monotonically decrease with increasing atomic number due to poor shielding between the nucleus and the $5s^25p^6$ valence shell by the 4f electrons (the lanthanide contraction),[58] and to a first approximation, metal ion hydrolysis constants are inversely proportional to ionic radii.[59] An additional factor is that the CN of lanthanide metal complexes, including hydrated lanthanide metal ions in bulk aqueous solution, change from nine for metals with small atomic numbers to eight for metals with large atomic numbers. For example, the partial molar volumes in aqueous solution and Pauling ionic radii for trivalent La, Pr, and Nd (CN = 9) are directly related, as are those quantities for Tb, Dy, Ho, Er, and Yb (CN = 8), but those for Sm and Gd show intermediate behavior, indicating variable CN (Eu was not included in that study, but lies between Sm and Gd in the lanthanide series).[60] This comparison indicates that the free energies of the eight- and nine-coordinate forms of trivalent Sm−Gd are very close and that the chemistry of these ions may be very sensitive to small changes in environment and interactions.

Infrared Action Spectra of Hydrated Trivalent Lanthanum. Infrared action spectra of selected $[M(H_2O)_n]^{3+}$ ions were measured for n near the turnover size and are shown in Figure 6. These spectra were measured in the free-OH region (3600−3760 cm^{-1}), which corresponds to the stretching modes of hydroxyl groups that do not donate a hydrogen bond. Many studies have shown that these bands are particularly useful for characterizing hydrated ion structure.[7–9,11,36,61,62] Hydrogen-stretch spectra acquired at lower frequencies, corresponding to hydroxyl groups that donate a hydrogen bond, can provide additional information, but this region of the spectrum can be challenging to interpret because of band broadening, spectral congestion, and other factors.[8,36,37] Because $[M(H_2O)_n]^{3+}$ readily dissociates due to ambient radiation alone under these conditions, the absorption of just one laser photon should cause observable photodissociation and the relative intensities in these action spectra should be very similar to those of true absorption spectra.

The spectra of $[M(H_2O)_n]^{3+}$ exhibit a four-band structure that is qualitatively similar to those observed for $[H(H_2O)_n]^+$.[7,8] These bands, marked using the notation of Shin et al.,[8] are attributable to nonbonded hydrogen stretches of water molecules in different hydrogen-bonding configurations, shown schematically in Figure 7. Bands *a* and *d* are assigned to the symmetric and asymmetric stretches of single-acceptor only water molecules (**A**, one-coordinate water), respectively, and bands *b* and *c* are assigned to the dangling-OH stretches of double-acceptor-single-donor (**AAD**, three-coordinate water) and single-acceptor-

(56) Reinhard, B. M.; Niedner-Schatteburg, G. *J. Chem. Phys.* **2003**, *118*, 3571–3582.
(57) Klungness, G. D.; Byrne, R. H. *Polyhedron* **2000**, *19*, 99–107.
(58) Seitz, M.; Oliver, A. G.; Raymond, K. N. *J. Am. Chem. Soc.* **2007**, *129*, 11153–11160.
(59) Baes, C. F.; Mesmer, R. E. *The Hydrolysis of Cations*; John Wiley and Sons: New York, 1976; pp 407−409.
(60) Spedding, F. H.; Pikal, M. J.; Ayers, B. O. *J. Phys. Chem.* **1966**, *70*, 2440–2449.
(61) Kamariotis, A.; Boyarkin, O. V.; Mercier, S.; Beck, R. D.; Bush, M. F.; Williams, E. R.; Rizzo, T. R. *J. Am. Chem. Soc.* **2006**, *128*, 905–916.
(62) Bush, M. F.; Prell, J. S.; Saykally, R. J.; Williams, E. R. *J. Am. Chem. Soc.* **2007**, *129*, 13544–13553.

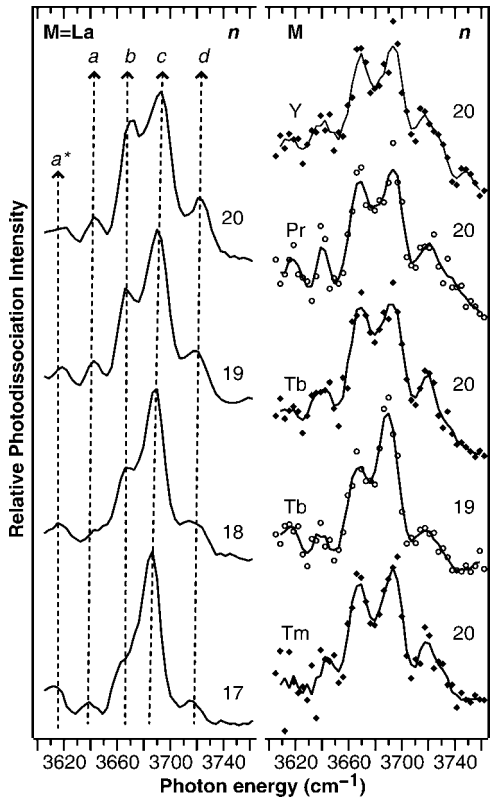

Figure 6. Infrared action spectra of $[M(H_2O)_n]^{3+}$, with M and n identified on the figure, obtained at a copper jacket temperature of 220 K. Both raw photodissociation data (markers) and a three-point average (line) are shown for M = Y, Pr, Tb, and Tm.[49]

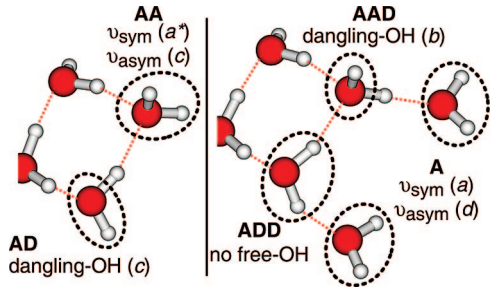

Figure 7. Acceptor (**A**) and donor (**D**) hydrogen-bonding configurations expected to contribute to the reported infrared spectra. The expected bands for each configuration are noted in lower-case italics and marked in Figure 6.

single-donor (**AD**, two-coordinate water) water molecules, respectively.[7,8] In addition, the infrared spectra of $[Ca(H_2O)_n]^{2+}$, $n \geq 8$, indicate that double acceptor-only water molecules (**AA**, Figure 7) are important hydrogen-bonding motifs in the solvation of hydrated multiply charged cations.[36] The asymmetric stretch of **AA** water molecules produces an intense band at a similar frequency to the dangling-OH stretch of the other two-coordinate motif (**AD**),[36] and the symmetric stretch is tentatively assigned to the lowest-frequency band (a*).

The four-band structure for $[La(H_2O)_n]^{3+}$ occurs at significantly lower frequencies than that for $[H(H_2O)_n]^+$, consistent with increased charge transfer from water molecules to higher charge-density cations.[11,36,63] On the basis of comparisons with the spectra reported previously for $[H(H_2O)_n]^+$,[7,8] and $[Ca(H_2O)_n]^{2+}$,[36] the increasing relative intensity of bands a, b, and d in the infrared spectra of $[La(H_2O)_n]^{3+}$ is most consistent with additional one- and three-coordinate water molecules, relative to two-coordinate water molecules, with increasing n. For example, if an **AD**-water molecule forms a new hydrogen bond to a free water molecule, the former would adopt an **ADD** configuration and exhibit no free-OH bands (band c depleted), whereas the later would adopt an **A** configuration and exhibit bands a and d (Figure 7). Alternatively, if an **AA**-water molecule forms a new hydrogen bond to a free water molecule, the former would adopt an **AAD** configuration exhibit band b (band c depleted), whereas the latter would adopt an **A** configuration and exhibit bands a and d (Figure 7).

The decreasing intensity of bands a and d, associated with one-coordinate water molecules, with decreasing n suggests that such water molecules may be fully depleted for $n \approx 16$. That cluster size may correspond to a tight, multishell core around trivalent lanthanum, to which additional water molecules bind in less favorable orientations. However, it is almost certain that multiple structures contribute to these infrared spectra and it is challenging to assign these spectra to specific structures. Disrupting water molecules involved in such a strongly bound core may be unfavorable, making hydrolysis of water a competitive process. Additionally, the activation barrier for hydrolysis may be reduced in the high-electric-field environment present in a minimally solvated, highly charged ion. If a salt-bridge structure is formed, the barrier to dissociation for hydrated H_3O^+ would be significantly lower than that for the loss of a water molecule due to Coulombic repulsion.[13]

Effect of Trivalent Metal Ion Identity on Hydrated Ion Structure. The spectra of $[M(H_2O)_{19}]^{3+}$ and $[M(H_2O)_{20}]^{3+}$ exhibit no discernible dependence on metal ion identity (Figure 6), even though the gas-phase turnover sizes and solution coordination numbers do. This suggests that the structures of $[M(H_2O)_n]^{3+}$, $n \approx 20$, are similar for all rare earth metal ions. The differences in gas-phase turnover sizes may be the result of subtle differences in activation energies for the two processes rather than significant differences in ion structure. Because dissociation in these BIRD experiments is kinetically controlled and likely occurs near threshold, branching ratios for Reaction 2 and Reaction 3 are likely to be extremely sensitive to even very small differences in the threshold dissociation energies for these two processes. The binding energy of a water molecule to the cluster increases with decreasing n in this size range. With decreasing n, the barrier to Reaction 2 increases, whereas the higher charge densities may lower the barrier to salt-bridge formation in Reaction 3.

It is also possible that there are subtle differences in structure that are not reflected by the IR spectra in the free-OH stretch region. Additional spectra in the bonded-OH stretch, water bend, or fingerprint regions may provide complementary information, but previous results for $[H(H_2O)_n]^+$[7−9] and $[Ni(H_2O)_n]^+$[11] indicate that spectra in the free-OH region are most sensitive to hydrated cation structure. Alternatively, the f−f electronic spectra of aqueous Nd^{3+}, $Ho,^{3+}$ and Er^{3+} are very sensitive to the number of coordinating ligands,[64] and the f−f electronic action spectra of hydrated trivalent metal ions in the gas phase may strongly complement these infrared spectra. Previously, d−d electronic action spectra of $[Co(H_2O)_{4-7}]^{2+}$ provided

(63) Cappa, C. D.; Smith, J. D.; Messer, B. M.; Cohen, R. C.; Saykally, R. J. *J. Phys. Chem. B* **2006**, *110*, 5301–5309.

(64) Karraker, D. G. *Inorg. Chem.* **1968**, *7*, 473–479.

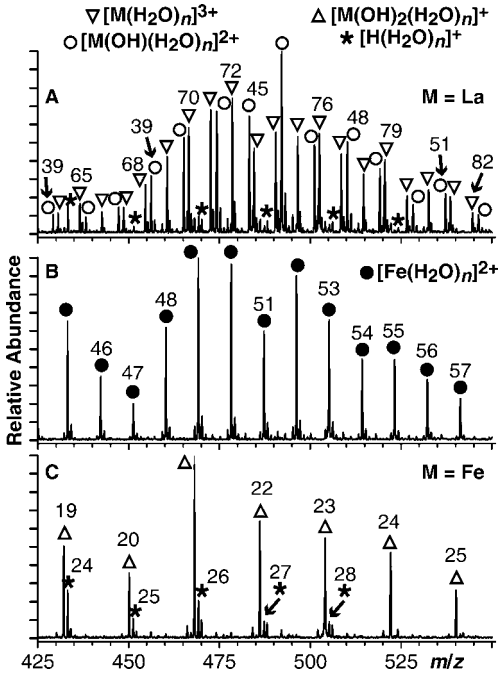

Figure 8. ESI mass spectra of $LaCl_3$ (A), $FeSO_4$ (B), and $FeCl_3$ (C) obtained in pure water under identical conditions.

insights into the temperature-dependent spectra of divalent cobalt in aqueous solution.[30]

Other Hydrated Trivalent Metal Ions. Under conditions which readily yield $[M(H_2O)_n]^{3+}$ ions for most lanthanide metals, ESI mass spectra of soutions containing M^{III} = Al, Cr, Fe, In, and Sc, exhibit no $[M(H_2O)_n]^{3+}$ ions. Charge-reduced ions and/or protonated water clusters are observed instead. For example, conditions that yield $[La(H_2O)_n]^{3+}$ ions from a La^{III} salt (Figure 8A) and $[Fe(H_2O)_n]^{2+}$ ions from an Fe^{II} salt (Figure 8B) yield only $[Fe(OH)_2(H_2O)_n]^+$ and $[H(H_2O)_n]^+$ ions from an Fe^{III} salt (Figure 8C).[65] Lowering the temperature of the stainless steel capillary increased the number of solvating water molecules[20] but did not affect the charge states of the ions observed.

The absence of $[M(H_2O)_n]^{3+}$, M = Al, Cr, Fe, In, and Sc, ions in these mass spectra is primarily attributable to the first hydrolysis constants of these metals in aqueous solution,[59] which indicate that the metals are predominantly hydrolyzed in pure aqueous solution. Addition of HCl at concentrations ranging from 100 μM to 1 M to the $FeCl_3$ electrospray solution increases the abundance of $[H(H_2O)_n]^+$ ions, but at the expense of signal for ions containing iron. Addition of weak acids, e.g., acetic acid, to the $FeCl_3$ electrospray solution increases the abundance of $[H(H_2O)_n]^+$ ions and new charge-reduced species containing the metal and the conjugate base of the weak acid, but neither $[Fe(OH)(H_2O)_n]^{2+}$ nor $[Fe(H_2O)_n]^{3+}$ were observed.

(65) Note that these experiments cannot distinguish between $[Fe(OH)_2(H_2O)_n]^+$ and $[FeO(H_2O)_{n+1}]^+$.

Conclusions

Electrospray ionization, BIRD, and infrared action spectroscopy have been used to form and characterize the structures and reactivities of hydrated trivalent rare earth metal ions in the gas phase. These ions dissociate by either the loss of one neutral water molecule (Reaction 2) or by the loss of a small protonated water cluster (Reaction 3). Relative rates for these two dissociation processes depend strongly on metal ion identity and cluster size. The transition from dissociation exclusively via Reaction 2 to exclusively via Reaction 3 occurs over a narrow range of cluster sizes that differ by only a few water molecules for each metal ion. Infrared action spectroscopy experiments indicate that for clusters with $n \approx 17-20$, over which this transition in reactivity occurs, single-acceptor only water molecules are depleted with decreasing n. Infrared action spectra of $[M(H_2O)_{19-20}]^{3+}$ exhibit no discernible dependence on metal ion identity, even though the gas-phase reactivities of these ions and solution coordination numbers do. These results suggest that any differences in ion structure may be very subtle and that the substantial differences in gas-phase reactivities exhibited by ions differing by as few as one water molecule may be attributable to very small differences in dissociation energy for Reactions 2 and 3.

Abundances of $[Yb(H_2O)_n]^{3+}$ were significantly lower than those observed for the other hydrated rare earth metals, even though the ionic radius of Yb is slightly larger than that of the smallest metal Lu.[58] Explaining the origin of the low abundances of $[Yb(H_2O)_n]^{3+}$ remains a topic of ongoing exploration and may provide additional insights into challenges of forming $[M(H_2O)_n]^{3+}$ for M outside of group III. In contrast to some previous studies of multiply charged metal ion clusters,[17,22,38,42–44,54,55] we find that the charge-separation chemistry of $[M(H_2O)_n]^{3+}$ does not depend directly on the ionization energy of the bare metal ion but does correlate well with the first hydrolysis constant in aqueous solution.

An important implication of these results, which indicate that trivalent lanthanide ions readily hydrolyze water when not surrounded by at least two solvent shells, is that ions that are weak acids in bulk solution, i.e., the lanthanide metals, which all have pK_a constants greater than that of water,[57] may have considerably greater propensities to hydrolyze water and biomolecules in environments that lack extended hydrogen bond networks and/or neighboring counterions. These conditions may be present in many important environments, including the interfaces between water and either air or membranes or in the cavities of large biomolecules.

Acknowledgment. The authors thank Professor Kenneth N. Raymond for helpful discussions and the National Science Foundation (Grants No. CHE-0718790 and CHE-0404571 for ERW and R.J.S., respectively) for generous financial support.

Supporting Information Available: Supporting Information Figure 1. This material is available free of charge via the Internet at http://pubs.acs.org.

JA801894D